Nanotechnology Perceptions
ISSN 1660-6795
www.nano-ntp.com

Effect Of Li-Co- Doping On The Structure And Optical Properties Of Sm^{3+} Doped PVP Capped $Mgal_2o_4$ Nanophosphors

Deepa Rani S*

Department of Physics, Government College for Women, Trivandrum, Kerala, India
**Corresponding author. Email:deeparanis1970@gmail.com*

In this study, rare earth ion (Sm^{3+}) doped and Li-co-doped magnesium aluminate ($MgAl_2O_4$) nanoparticles were synthesized using polymerised sol-gel combustion method. A series of trivalent Samarium (Sm^{3+}) activated magnesium aluminate nanophosphors ($Mg_{1-x}Sm_xAl_2O_4$ (x = 0.02, 0.04, 0.06, 0.08 and 0.10)) and Li-co-doped $MgAl_2O_4$: Sm^{3+}nanophosphors were synthesized and their structural, optical and luminescence properties were studied using different characterization techniques such as X-ray diffraction (XRD), Fourier transform infrared spectra (FTIR), Diffuse reflectance spectra (DRS), X-ray photoelectron spectroscopy (XPS) and photoluminescence (PL) spectroscopy.The polymer used was polyvinylpyrrolidone(PVP) which acted as a reducing agent and stabilizing agent during synthesis. The average crystallite size,which was estimated from the x-ray diffraction analysis of all prepared nanophosphors,was around 10 nm. FTIR spectra showed various fingerprint bands in the range 400-700 cm^{-1}. DRS spectra showed strong absorption in the UV region at 401 nm.XPS analysis confirmed the presence of different elements in the prepared nanophosphors. Photoluminescence emission spectra showed many characteristic peaks in the visible region for all samples upon 401 nm excitation. The most prominent peak was at 649 nm wavelength corresponding to the $^4G_{5/2} - {}^6H_{9/2}$ transition. Li-co-doping enhances the emission intensity by almost 1.98 % without change in the peak positions. The results suggest that the synthesized nanophosphors could be an excellent choice for orange-red emitting luminescent materials for UV-excited phosphor-converted white light-emitting diodes and for various photonic applications.

Key words: Nanophosphors; Sol-gel; FTIR; Co-doping.

1. Introduction

The huge demand for luminescent materials in display and optical applications led to the development of nanomaterials activated by lanthanide ions [1]. Inorganic phosphors based on oxide systems are excellent choices due to their low toxic level,high mechanical strength, high melting point, high resistance to chemical attacks, their excellent dielectric and optical properties, and the absence of radioactive elements. When rare earth ions are incorporated into suitable hosts, the nanophosphors obtained can produce intense narrow emissions due to 4f shell electronic transitions. A prominent rare earth ion which produces intense reddish orange light is Samarium (Sm^{3+}) [1]. Magnesium aluminate ($MgAl_2O_4$) with spinel structure is considered to be the most reliable host material due to many attractive properties like wide

band gap, stable thermal and chemical properties, excellent dielectric and optical properties, and the absence of radioactive elements. Suitable rare earth elements doped into $MgAl_2O_4$ can serve as excellent nanophosphors for photonic applications[2-4].Structural and optical properties are greatly influenced by the method of synthesis of the nano materials.Here, the polymerised sol-gel combustion method was employed to synthesize Sm^{3+} doped nanophosphors.The polymer used,polyvinylpyrrolidone(PVP), controlled the size and acted as a surface capping agent during the synthesis[5].In this paper, a series of samarium-doped magnesium aluminate phosphors ($Mg_{1-x}Sm_xAl_2O_4$ (x = 0.02, 0.04, 0.06, 0.08 and 0.10)) and Li-co-doped $MgAl_2O_4$: Sm^{3+} nanophosphors were synthesized using polymerised sol-gel combustion method. The influence of Sm^{3+} ion concentration on the structural and optical properties of synthesized nanophosphors was analyzed in detail. It was noticed that Li-co-doping enhanced the photoluminescence efficiency of the nanophosphors.The addition of co-dopant ions increased the crystallinity and removed the charge imbalance problem in the synthesized nanophosphors.

2. Materials and methods

Samarium-dopedmagnesium aluminate nanophosphors and Li-co-doped $MgAl_2O_4$: Sm^{3+}nanophosphors were synthesized using polymerised sol-gel combustion method. The materials used for the synthesis were magnesium nitrate hexahydrate ($Mg(NO_3)_2.6H_2O$,99.99%, Sigma-Aldrich), samarium (III) nitrate hexahydrate ($Sm(NO_3)_3.6H_2O$,99.99%, Sigma-Aldrich), aluminium nitrate nonahydrate ($Al(NO_3)_3.9H_2O$, 99.9%, Merck), citric acid ($C_6H_8O_7$, 99.9%, Merck), lithium nitrate ($LiNO_3$, 99.99%, Sigma-Aldrich) and polyvinylpyrrolidone ($(C_6H_9NO)n$, 40000 g/mol, 99%, Sigma-Aldrich).Stoichiometric amounts of magnesium nitrate, aluminium nitrate and samarium nitrate were dissolved in deionized water and stirred continuously for one hour in a magnetic stirrer. The metal nitrate to citric acid ratio was maintained as 1:2. To this nitrate solution, citric acid was added dropwise to form the metal-citrate solution. To this mixture, 1 wt% PVP solution was added and stirred continuously for three hours to form a homogeneous polymerised complex. To one part of the prepared solution, 2 % lithium nitrate was added and stirred continuously for two more hours. The resultant precursors were then kept in a hot air oven at 120 ^{O}C for twelve hours until a yellowish dried xerogel was obtained. The dried gel was then subjected to controlled combustion at 350^{O}C in a muffle furnace.The resultant powder was then finely ground and kept in a muffle furnace at 900^{O}C for five hours to obtain $Mg_{1-x}Sm_xAl_2O_4$ (x = 0.02, 0.04, 0.06, 0.08 and 0.10) nanophosphors and Li-co-doped $MgAl_2O_4$: Sm^{3+} nanophosphors.

To study the crystal structure and to identify the formation of phase in the synthesized phosphors, X-ray diffraction (XRD) measurements were carried out on a Bruker (D8 ADVANCE DAVINCI) X-ray diffractometer using CuKα radiation (1.54056 Å) in the angular range (2θ) of 10^{O}to 70^{O}. The Fourier transform infrared spectra (FTIR) of the prepared samples were monitored in the wave number range 400-4000 cm^{-1} by a Fourier Transform Infrared (FTIR) Spectrometer (Perkin Elmer Spectrum Two FT-IR Spectrometer) employing the KBr pellet method. Diffuse reflectance spectra were carried out on a UV-visible NIR spectrophotometer (JASCO V-750) with $BaSO_4$ as the reference. X-ray photoelectron spectroscopy (XPS) measurements were carried out to analyze the surface properties and

oxidation states of the elements using an X-ray photoelectron spectrometer (Thermo Scientific ESCALAB XI^+ A1528) integrated with AlKα (1486.6 eV) source (X-ray spot size of 900µm).Photoluminescence excitation and emission spectra of the samples were recorded using a HORIBA SCIENTIFIC FLUOROLOG 3 spectrofluorometer,witha 450 W Xenon lamp as the excitation source.

3. Results and discussion

3.1 X-ray diffraction study

The X-ray diffraction patterns of $Mg_{1-x}Sm_xAl_2O_4$ (x = 0.02, 0.04, 0.06, 0.08 and 0.10) nanophosphors and Li-co-doped $MgAl_2O_4$: Sm^{3+} nanophosphors are shown in Fig. 1.All the diffraction peaks matched well with the cubic spinel phase of $MgAl_2O_4$ and were indexed according to the ICDD File No. 01-070-5187 (Space group Fd-3m (227), cubic system).The absence of impure phases in the pattern suggests that doping and co-doping of dopants in $MgAl_2O_4$ did not change the phase, and indicates successful incorporation of Sm^{3+} ions and Li^+ ions in the crystal lattice.The peaks depict the high crystallinity of the samples and the crystallite sizes were estimated by the Debye-Scherrer equation [6],

$$\text{Crystallite size (D)} = \frac{k\lambda}{\beta_{hkl}\cos\theta_{hkl}} \quad (1)$$

where k is a dimensionless shape factor (= 0.9), λ is the X-ray wavelength used (CuKα =1.54056 Å), β is the full widthat half the maximum intensity (FWHM) of the diffraction peaks in radian, θ is the Bragg diffraction angle and D is the crystallite size along (hkl)direction. The average crystallite sizes decreased slightly with the increase in the concentration of Sm^{3+} ions, and were estimated as12.60, 10.58, 9.59, 8.71, 8.29 and 10.27 nm for $Mg_{1-x}Sm_xAl_2O_4$(x = 0.02, 0.04, 0.06, 0.08 and 0.10) and Li-co-doped $MgAl_2O_4$: Sm^{3+}nanophosphors.Due to the closeness in the ionic radii of Mg^{2+}(0.072 nm) and Li^+ (0.068 nm), Li^+ easily substitutes Mg^{2+} in the $MgAl_2O_4$ lattice[6, 7].

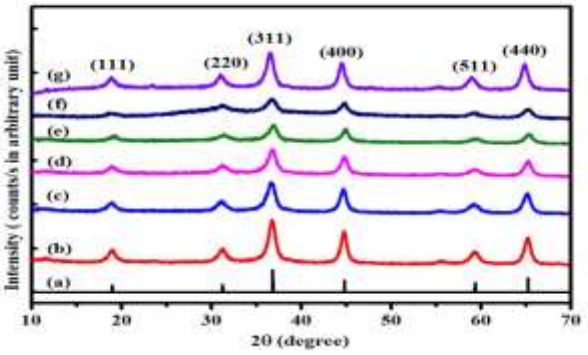

Fig.1 X-ray diffraction patterns (a) $MgAl_2O_4$ standard data; $Mg_{1-x}Sm_xAl_2O_4$ nanophosphors with different Sm^{3+} content (x) (b) 0.02, (c) 0.04, (d) 0.06, (e) 0.08 (f), 0.10 and (g) $Mg_{0.96}Sm_{0.04}Al_2O_4$: Li^+ nanophosphors.

3.2 Optical studies

Formation of pure phase $Mg_{1-x}Sm_xAl_2O_4$(x = 0.02, 0.04, 0.06, 0.08 and 0.10) and Li-co-doped $MgAl_2O_4$: Sm^{3+}nanophosphors have been confirmed by monitoring FTIR spectra taken in the range 400 to 4000 cm^{-1}. Fig. 2 depicts the FTIR spectra of the prepared samples which shows similar finger print bands in all samples centered around 488 $cm^{-1}$and 670cm^{-1}, which corresponds to the stretching vibrations of AlO_6 octahedral groups and Mg-O in $MgAl_2O_4$[8, 9].

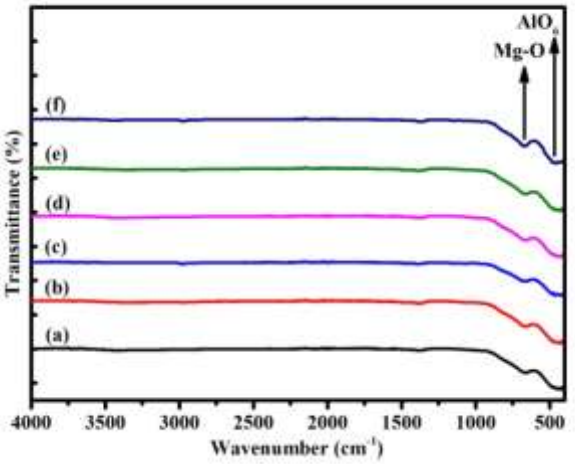

Fig.2: Fourier transform infrared spectra of $Mg_{1-x}Sm_xAl_2O_4$ nanophosphors with different Sm^{3+} content (x) (a) 0.02, (b) 0.04, (c) 0.06, (d) 0.08, (e) 0.10 and (f) $Mg_{0.96}Sm_{0.04}Al_2O_4$: Li^+ nanophosphors.

Diffuse reflectance spectra of $Mg_{1-x}Sm_xAl_2O_4$ (x = 0.02, 0.04, 0.06, 0.08 and 0.10) and Li-co-doped $Mg_{0.94}Sm_{0.06}Al_2O_4$ nanophosphors measured in the wavelength range 200 to 500 nm are depicted in Fig. 3 and 4. All the samples exhibit similar spectral profile with a prominent and strong absorption at 401 nm which corresponds to $^6H_{5/2} \rightarrow {}^4F_{7/2}$ transition of Sm^{3+} ions [10, 11]. Absorption intensity tends to increase with the increase in the concentration of dopant ions.

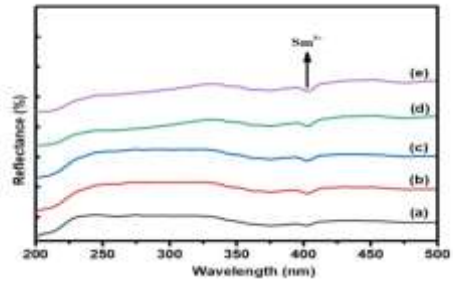

Fig.3: UV-Vis diffuse reflectance spectra of $Mg_{1-x}Sm_xAl_2O_4$ nanophosphors with different Sm^{3+} concentration (x) (a) 0.02, (b) 0.04, (c) 0.06, (d) 0.08 and (e) 0.10

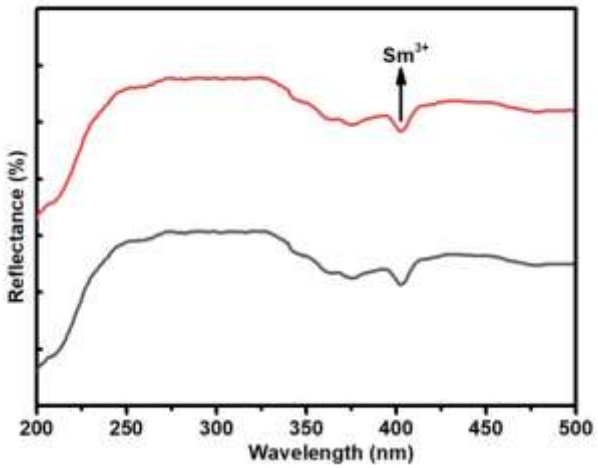

Fig.4: UV-Visible diffuse reflectance spectra of $Mg_{0.96}Sm_{0.04}Al_2O_4$ and $Mg_{0.96}Sm_{0.04}Al_2O_4$: Li^+ nanophosphor.

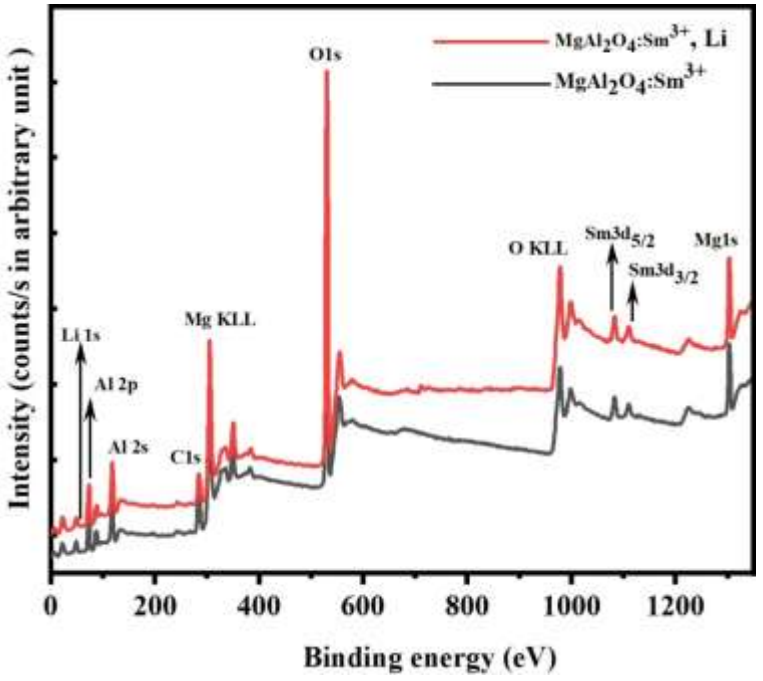

Fig.5 XPS survey scan of $Mg_{0.96}Sm_{0.04}Al_2O_4$ and Li- co-doped $Mg_{0.96}Sm_{0.04}Al_2O_4$ nanophosphors.

X-ray photoelectron spectroscopic technique (XPS) was utilised as one of the most prominent methods to understand the chemical bonding characterization in compounds.Fig. 5 shows the XPS survey spectrum of the $Mg_{0.96}Sm_{0.04}Al_2O_4$ and $Mg_{0.96}Sm_{0.04}Al_2O_4$: Li^+ nanophosphor which shows the presence of Mg^{2+}, Al^{3+}, O, Sm^{3+} and Li^+ions in the prepared samples. The measured XPS spectra were charge-corrected using the core level carbon peak C1s of the adventitious carbon at 284.6 eV as the reference. The photoelectric peak of Mg1s was obtained at 1305.98 eV, indicating the presence of magnesium as oxide in the sample. The peak centered at 72.64 eV was assigned to Al2p, which is due to the presence of Al^{3+} cations bonded to oxygen as Al-O bonds in the oxide spinel structure. The symmetrical photoelectron peak obtained at 530.95 eV was associated with O1s level, which indicates the presence of only one kind of oxygen species in the synthesized phosphor. The Sm3d core level spectra showed a doublet structure with an energy separation of 26.17 eV, ascribed to $Sm3d_{3/2}$ and $Sm3d_{5/2}$ which arose due to spin-orbit interaction, and was obtained at binding energies of 1109.61 and 1083.44 eV.XPS spectra is similar for Li-co-doped $Mg_{0.96}Sm_{0.04}Al_2O_4$ except, the spectra shows the presence of Li^+ ions around 56 eV [12, 13].

3.3 Photoluminescence study

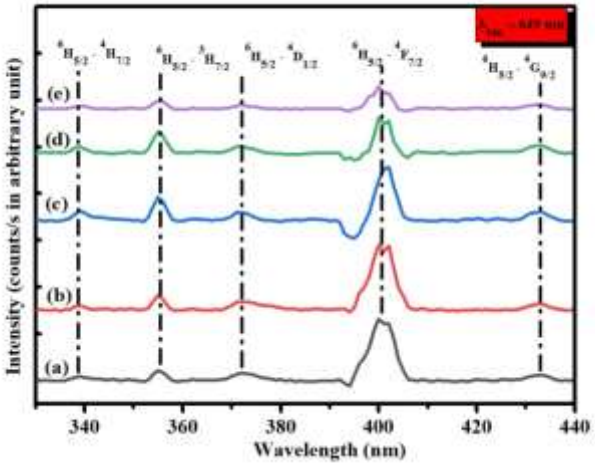

Fig. 6: Excitation spectra (λ_{em}= 649 nm) of $Mg_{1-x}Sm_xAl_2O_4$ nanophosphors with different Sm^{3+} content (x) (a) 0.02, (b) 0.04, (c) 0.06, (d) 0.08 and (e) 0.10.

Samarium-doped nanophosphors are efficient light emitters in the reddish orange region under UV excitation. The excitation spectrum recorded at 649 nm emission of $Mg_{1-x}Sm_xAl_2O_4$(x = 0.02, 0.04, 0.06, 0.08 and 0.10) nanophosphor is shown in Fig. 6. The most intense peak at 401nm is ascribed as $^6H_{5/2} - {}^4F_{7/2}$, the characteristic f-f transition of Sm^{3+} ions from ground state to excited state. The excitation spectrum exhibited several other peaks originating from $^6H_{5/2}$to several excited states located at 339, 355, 372, and 433 nm corresponding to the transitions $^6H_{5/2} - {}^4H_{7/2}$, $^6H_{5/2} - {}^3H_{7/2}$, $^6H_{5/2} - {}^4D_{1/2}$ and $^6H_{5/2} - {}^4G_{9/2}$ [14,15].Fig.7 shows the

excitation spectra of $Mg_{0.96}Sm_{0.04}Al_2O_4$ and Li- co-doped $Mg_{0.96}Sm_{0.04}Al_2O_4$ nanophosphor, which shows the excitation peaks at the same wavelengths except the enhancement in the intensity of peaks due to Li-co-doping[16].The obtained maximum intensity peak at 401 nm in $Mg_{1-x}Sm_xAl_2O_4$ (x = 0.02, 0.04, 0.06, 0.08 and 0.10) nanophosphors suggests that they can be successfully excited by near UV LED's for photonic applications.

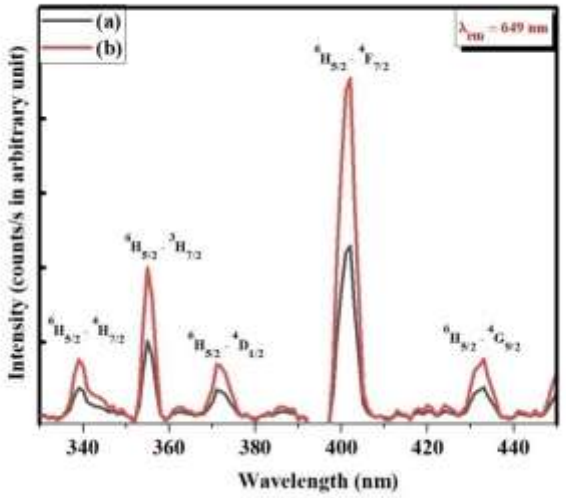

Fig.7: Excitation spectra (λ_{em}= 649 nm) of (a) $Mg_{0.96}Sm_{0.04}Al_2O_4$ and (b) $Mg_{0.96}Sm_{0.04}Al_2O_4$: Li^+ nanophosphor.

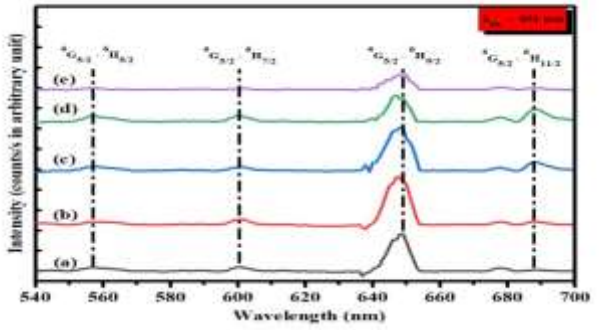

Fig.8: Emission spectra (λ_{ex}= 501 nm) of $Mg_{1-x}Sm_xAl_2O_4$ nanophosphors with different Sm^{3+} content (x) (a) 0.02, (b) 0.04, (c) 0.06, (d) 0.08 and (e) 0.10.

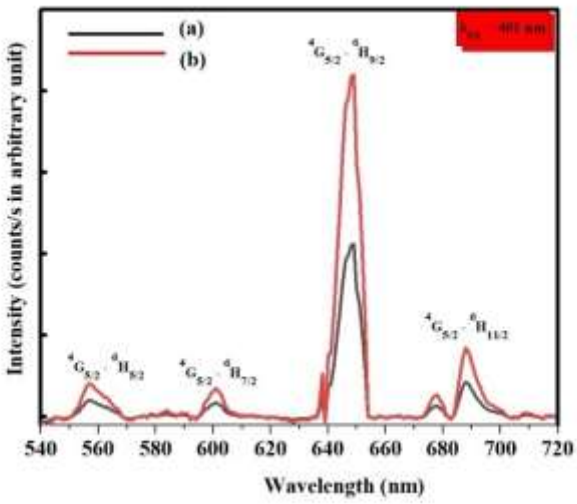

Fig.9: Emission spectra (λ_{ex}= 401nm) of (a) $Mg_{0.96}Sm_{0.04}Al_2O_4$ and (b) $Mg_{0.96}Sm_{0.04}Al_2O_4$: Li^+ nanophosphor.

The photoluminescence emission spectra of $Mg_{1-x}Sm_xAl_2O_4$ (x = 0.02, 0.04, 0.06, 0.08 and 0.10) nanophosphors recorded at 401 nm excitation wavelength show characteristic peaks corresponding to the electronic transitions of the Sm^{3+} system. The spectra, shown in Fig. 8, depicts four peaks centered at 556, 600, 649 and 688 nm identified as $^4G_{5/2} - {}^6H_{5/2}$, $^4G_{5/2} - {}^6H_{7/2}$, $^4G_{5/2} - {}^6H_{9/2}$ and $^4G_{5/2} - {}^6H_{11/2}$ transitions. The most intense transition is at 649 nm, corresponding to the transition $^4G_{5/2} - {}^6H_{9/2}$ of Sm^{3+} ions, which is a purely electric dipole transition and is sensitive to the crystal field. The optimum concentration of Sm^{3+} ions is 4 mol. % beyond which the emission intensity decreases due to concentration quenching phenomenon. The cross- relaxation between the neighbouring Sm^{3+} ions as the concentration increases leads to the concentration quenching effect resulting in a decrease in intensity[17-23].The luminescence characteristics of $Mg_{1-x}Sm_xAl_2O_4$ (x = 0.02, 0.04, 0.06, 0.08 and 0.10) nanophosphors mark their suitability for applications in near-ultraviolet excited phosphor converted white light emitting diodes.

Fig. 9 depicts the photoluminescence emission spectra of $Mg_{0.96}Sm_{0.04}Al_2O_4$ and $Mg_{0.96}Sm_{0.04}Al_2O_4$: Li^+ sample, which show the emission peaks at the same wavelength with increase in emission intensity. Li^+ ions acted as sensitizers helping the energy transfer from the host to Sm^{3+} active centres, which improved the photo luminescence characteristics of the lithium doped nanophosphor. The charge compensation achieved by the addition of Li ions, led to the enhancement in the photo luminescence intensity to almost two times [16, 24].

Conclusions

Spinel structured $Mg_{1-x}Sm_xAl_2O_4$ (x = 0.02, 0.04, 0.06, 0.08 and 0.10) nanophosphors and Li-co-doped $MgAl_2O_4$:Sm^{3+} nanophosphor was synthesized by polymerised sol-gel combustion

method. The average crystallite size calculated using Debye-Scherrer formula was found be in the range 8 to 13 nm. The polymer,polyvinylpyrrolidonePVP, played a significant role in the synthesis by acting as a surface capping agent, controlling the growth of the prepared nanophosphors. FTIR spectra exhibited the different functional groups present in the samples. DRS spectra showed maximum absorption in the UV region at 401nm. Photoluminescence excitation and emission spectra showed sharp peaks corresponding to the 4f-4f transitions of Sm^{3+} ions. Excitation spectra monitored at 649 nm emission showed several peaks of varying intensities with $^6H_{5/2} - {}^4F_{7/2}$ (401 nm) transition as the most intense. The doped samples showed the emission peaks at 556, 600, 649 and 688 nm corresponding to $^4G_{5/2} - {}^6H_{5/2}$, $^4G_{5/2} - {}^6H_{7/2}$, $^4G_{5/2} - {}^6H_{9/2}$ and $^4G_{5/2} - {}^6H_{11/2}$ transitions, with $^4G_{5/2} - {}^6H_{9/2}$ (649 nm) transition having maximum intensity. The optimum doping concentration was found to be at 4 mol. %, after which photoluminescence intensity decreased due to concentration quenching.Further, it was established that Li-co-doping enhanced the emission intensity considerably. The emission spectrum produced at 401 nm excitation showed intense orange- red emission, indicating that the prepared nanophosphors are capable of functioning as red emitters for white LEDs in solid state lighting applications.

References

1. Shivaram, M., et al. "Synthesis and luminescence properties of Sm^{3+} doped $CaTiO_3$ nanophosphor for application in white LED under NUV excitation." Spectrochimica Acta Part A: Molecular and Biomolecular Spectroscopy 128 (2014): 891-901 http://dx.doi.org/10.1016/j.saa.2014.02.117
2. Ganesh, Int. "A review on magnesium aluminate ($MgAl_2O_4$) spinel: synthesis, processing and applications." International Materials Reviews 58.2 (2013): 63-112.https://doi.org/10.1179/1743280412Y.0000000001
3. Perkins, J. M., G. D. West, and M. H. Lewis. "Analysis and spectroscopy of rare earth doped magnesium aluminate spinel." Advances in applied ceramics 104.3 (2005): 131-134.https://doi.org/10.1179/174367605X20162
4. Koczkur, Kallum M., et al. "Polyvinylpyrrolidone (PVP) in nanoparticle synthesis." Dalton transactions 44.41 (2015): 17883-17905.https://doi.org/10.1039/C5DT02964C
5. Shao, Huiping, et al. "Effect of PVP on the morphology of cobalt nanoparticles prepared by thermal decomposition of cobalt acetate." Current Applied Physics 6 (2006): e195-e197.https://doi.org/10.1016/j.cap.2006.01.038
6. Pratapkumar, C., Prashantha, S. C., Nagabhushana, H., &Jnaneshwara, D. M. (2018). Photoluminescence and photometric studies of low temperature prepared red emitting MgAl2O4: Cr3+ nanophosphors for solid state displays. Journal of Science: Advanced Materials and Devices, 3(4), 464-470.https://doi.org/10.1016/j.jsamd.2018.09.002
7. Wiglusz, R. J., et al. "Preparation and spectroscopy characterization of Eu: $MgAl_2O_4$nanopowder prepared by modified Pechini method." Journal of nanoscience and nanotechnology 9.10 (2009): 5803-5810.https://doi.org/10.1166/jnn.2009.1259
8. Kolesnikov, I. E., et al. "Structural and luminescence properties of $MgAl_2O_4$: Eu^{3+}nanopowders." Journal of Alloys and Compounds 654 (2016): 32-38.https://doi.org/10.1016/j.jallcom.2015.09.122
9. Eslami, A., Lachini, S. A., Shaterian, M., Karami, M., &Enhessari, M. (2024). Sol-gel synthesis, characterization, and electrochemical evaluation of magnesium aluminate spinel nanoparticles for

high-capacity hydrogen storage. Journal of Sol-Gel Science and Technology, 109(1), 215-225. https://doi.org/10.1007/s10971-023-06260-1

10. Nantharak, Worawut, et al. "Effect of local structure of Sm3+ in MgAl2O4: Sm3+ phosphors prepared by thermal decomposition of triethanolamine complexes on their luminescence property." Journal of Alloys and Compounds 701 (2017): 1019-1026.https://doi.org/10.1016/j.jallcom.2017.01.090
11. V. M. Maphiri, B. F. Dejene, T. E. Motaung, Thulani Thokozani Hlatshwayo, O. M. Ndwandwe, S. V. Motloung, The effects of varying the Eu^{3+} concentration on the structural and optical properties of $Mg_{1.5}Al_2O_{4.5}$: x% Eu^{3+} ($0 \leq x \leq 2$) nanophosphors prepared by sol–gel method, Nanomater. Nanotechnol. 8 (2018) 1847980418800644. https://doi.org/10.1177/1847980418800644.
12. Prakashbabu, D., et al. "Charge compensation assisted enhancement of photoluminescence in combustion derived Li^+ co-doped cubic ZrO_2: Eu^{3+} nanophosphors." Physical Chemistry Chemical Physics 18.42 (2016): 29447-29457.https://doi.org/10.1039/C6CP04633A
13. Khajuria, Pooja, et al. "Surface and spectral investigation of Sm^{3+} doped MgO-ZrO_2 phosphor." Optik 216 (2020): 164909.doi.org/10.1016/j.ijleo.2020.164909
14. Kumar, Sandeep, et al. "Synthesis and spectral properties of Sm^{3+} doped $MgAl_2O_4$ phosphor." AIP Conference Proceedings. Vol. 2220. No. 1. AIP Publishing, 2020. https://doi.org/10.1063/5.0001443
15. Bele, A., et al. "Effects of varying Sm^{3+} concentration on the structure, morphology and photoluminescence properties of the $BaAl_2O_4$/$CaAl_2O_4$/$Ca_4Al_6O_{13}$/$Ca_3Al_2O_6$: x% Sm^{3+} (0 x 1.9) mixed phases using citrate sol-gel method." https://doi.org/10.1016/j.heliyon.2022.e12573
16. Yadav, R. S., Yadav, R. V., Bahadur, A., Yadav, T. P., & Rai, S. B. (2016). Role of Li^+ on white light emission from Sm3+ and Tb3+ co-doped Y2O3 nano-phosphor. Materials Research Express, 3(3), 036201.DOI 10.1088/2053-1591/3/3/036201
17. Damini, R., et al. "Structural and photoluminescence of Sm^{3+} doped La_2O_3 nanophosphor." AIP Conference Proceedings. Vol. 2274. No. 1. AIP Publishing, 2020. https://doi.org/10.1063/5.0022388
18. Yashodha, S. R., N. Dhananjaya, and C. Manjunath. "Synthesis and photoluminescence properties of Sm^{3+} doped LaOCl phosphor with reddish orange emission and it's Judd-Ofelt analysis." Materials Research Express 7.1 (2019): 015003., DOI 10.1088/2053-1591/ab57a6
19. Yang, Hyun Kyoung, et al. "Crystal growth and photoluminescence properties of Sm^{3+} doped CeO_2 nanophosphors by solvothermal method." Journal of Nanoscience and Nanotechnology 13.9 (2013): 6060-6063. https://doi.org/10.1166/jnn.2013.7648
20. Chen, Y., Yang, H., Chung, J., Moon, B., Choi, H., Jeong, J., & Kim, J. (2010). Luminescence properties and crystallinity of Sm 3+-doped NaGd (WO 4) 2 powder phosphors. Journal of the Korean Physical Society, 57(61), 1760-1763.
21. Guo, Heng, et al. "A novel Sm^{3+} singly doped $LiCa_3ZnV_3O_{12}$ phosphor: a potential luminescent material for multifunctional applications." RSC advances 8.58 (2018): 33403-33413. https://doi.org/10.1039/C8RA07329E
22. Pratibha, S., N. Dhananjaya, and R. Lokesh. "Investigations of enhanced luminescence properties of Sm^{3+} doped $LaAlO_3$ nanophosphors for field emission displays." Materials Research Express 6.12 (2020): 1250c7. DOI10.1088/2053-1591/ab6381
23. Mahajan, Rubby, et al. "Synthesis and luminescent properties of Sm^{3+} doped zinc aluminate phosphor." AIP conference proceedings. Vol. 1953. No. 1. AIP Publishing, 2018. https://doi.org/10.1063/1.5032544

24. Tan, Y., Yan, Y., Du, H., Hu, X., Li, G., Kuang, Y, & Guo, D. (2018). Enhanced luminescence via Li+ doping from a Sm3+/Eu3+ Co-doped cerium oxide phosphor. Optical Materials, 85, 538-544.https://doi.org/10.1016/j.optmat.2018.09.012
.